On the Range of Frequencies of Intrinsic Climate Oscillations

Anastasios A. Tsonis and Michael D. Madsen

Abstract The purpose of this work is to establish the limits of natural oscillations in the climate system, i.e., not attributed to alleged anthropogenic effects. To this end we considered many proxy climate records representing the state of climate in the past when human activity was not a factor.

Keywords Climate oscillations • Natural variability

1 Introduction and Data

Twenty different reconstructed short-length proxy temperature records, six instrumental temperature records as well as five long-length proxy temperature records (four of which are ice-core reconstructed temperature records and the other reconstructed temperature record being from marine benthic oxygen isotopes) were analyzed in this study. The twenty reconstructed proxy temperature records represent annual means and range in length, location, and type. The six instrumental temperature records are monthly mean records and were all located in central Europe. They range in length from 231 to 247 years. Four of the long proxies are ice cores and one is a global marine benthic oxygen isotope record. Three of them have uneven time interval, while in two of them the values are spaced 500 years apart.

The details of the records used in this paper are as follows: Laguna Aculeo, Chile, summer mean sediment pigments, (856–1997 AD) (Von Gunten et al. 2009); Baffin Island, Canada, summer mean sediment thickness, (752–1992 AD) (Moore et al. 2003); Canadian Rockies, Canada, summer mea tree-ring thickness, (950–1994 AD) (Luckman and Wilson 2006); Firth, Alaska, summer mean tree-ring thickness,

A.A. Tsonis (✉)
Department of Mathematical Sciences, Atmospheric Sciences Group, University of Wisconsin - Milwaukee, Milwaukee, WI, USA

Hydrologic Research Center, San Diego, CA, USA
e-mail: aatsonis@uwm.edu

M.D. Madsen
Department of Mathematical Sciences, Atmospheric Sciences Group, University of Wisconsin - Milwaukee, Milwaukee, WI, USA

© Springer International Publishing AG 2018

A.A. Tsonis (ed.), *Advances in Nonlinear Geosciences*,
DOI 10.1007/978-3-319-58895-7_30

aatsonis@uwm.edu

(1073–2002 AD) (Anchukaitis et al. 2013); Canadian Rockies, tree-ring thickness (950–1994 AD) (Luckman and Wilson 2006); Iceberg Lake, Alaska, annually varve thickness, (442–1998 AD) (Loso 2008); Gulf of Alaska, summer mean tree-ring thickness, (724–1999 AD) (Wilson et al. 2007); Idaho, USA, annually July mean tree-ring thickness, (1135–1992 AD) (Biondi et al. 2006); North Andes, South America, annual mean tree-ring thickness, 1640–1987 AD), South Andes, South America, annual mean tree-ring thickness, (1640–1993 AD) (Villalba et al. 2006); Beijing, China, summer mean stalagmite thickness, (−665–1985 AD) (Tan et al. 2003); Central Europe, annual mean documentary data, (1005–2001 AD) (Glaser and Riemann 2009); China, annual multi-proxy reconstruction, (1000–1950 AD) (Shi et al. 2012); Cold Air Cave, South Africa, 5-year smoothed annual stalagmite isotope, (1635–1993 AD) (Sundqvist et al. 2013); European Alps, summer mean tree-ring and sediment thickness, (1053–1996 AD) (Trachsel et al. 2012); Lake Silvaplana, Switzerland, summer mean visible reflectance spectroscopy of lake sediment, (1175–1949 AD) (Trachsel et al. 2010); Slovakia, Europe, summer mean tree-ring, (1040–2011 AD) (Büntgen et al. 2013); Sweden, Europe, summer mean tree-ring, (1107–2007 AD) (Gunnarson et al. 2011); Tornetrask, Sweden, annual tree-ring, (500–2004 AD) (Grudd 2008); West Qinling Mts., China, annual tree-ring, (1500–1995 AD) (Yang et al. 2013); Spannagel Cave, Europe, stalagmite thickness, (-9–1935 AD) (Mangini et al. 2005); Paris, France, monthly mean instrumental, (1764–2000 AD) (Météo France 2012); Hohenpeißenberg, Germany, monthly mean instrumental, (1781–2013 AD) (Climate Research Unit CRU 2012); Kremsmunster, Austria, monthly mean instrumental, (1767–2013 AD) (Auer et al. 2007); Munich, Germany, monthly mean instrumental, (1781–2011 AD) (Deutscher Wetterdienst DWD 2012); Prague, Austria, monthly mean instrumental, (1771–2013 AD) (Czech Hydrometeorological Institute CHMI 2012); Vienna, Austria, monthly mean instrumental, (1775–2013 AD) (Climate Research Unit CRU 2012); Dome Fuji, Antarctica, ice core, (−339500–750 AD) (Kawamura et al. 2007); EPICA Dome C, Antarctica, ice core, (−800,000–1900 AD) (Jouzel et al. 2007); GISP2 ice core, central Greenland, ice core, (−48000–1850 AD) (Alley 2004); Global 1Ma Temperature, marine benthic oxygen isotopes, (−1067900–2000 AD) (Bintanja et al. 2005); Vostok, Antarctica, ice core, (−470766–2000 AD) (Petit et al. 1999).

For the analysis here, all six instrumental monthly records were converted to yearly mean records. The uneven records were interpolated to fill in missing values and to create 500-year-interval records. For interpolation we employed the piecewise cubic spline interpolation function in Matlab® (interp1).

2 Method and Results

In this study, we used the simple method of discrete Fourier transform (DFT) as our method for spectral analysis. DFT converts finite, equal spaced time domain samples, temperature records, into a finite combination of complex sinusoids ordered by their frequencies. Note that interpolation can result in enhancing lower frequencies and reducing higher frequency components (Schulz and Mudelsee 2002). To verify

aatsonis@uwm.edu

that our interpolation has little to no effect on the frequency components, our interpolated temperature records' DFT spectral analyses are compared to the spectral analysis using the Lomb–Scargle periodogram method. We found that both peak frequency and intensity are comparable between the two methods.

Each temperature record used in this study was first detrended using the Matlab® function (detrend). In order to obtain more frequency steps in the DFT spectral analysis, zero padding was applied to both ends of the temperature records to create temperature records of equal length of $N = 10000$ time steps. Then for each temperature record we employed the discrete Fourier transform using the fast Fourier transform function in Matlab® (fft). The output of this function was a combination of complex sinusoids in the form $A + Bi$, where A and B are a pair of harmonic predictors which can be found using:

$$A_k = \frac{2}{N}\sum_{i=1}^{N} y_i \cos\frac{2\pi k i \Delta t}{T}$$

$$B_k = \frac{2}{N}\sum_{i=1}^{N} y_i \sin\frac{2\pi k i \Delta t}{T}$$

$$\text{for}: k = 1, \frac{N}{2} - 1$$

$$A_{\frac{N}{2}} = \frac{1}{N}\sum_{i=1}^{N} y_i \cos\frac{\pi N i \Delta t}{T}$$

$$A_0 = \frac{1}{N}\sum y_i$$

$$B_0 = B_{\frac{N}{2}} = 0$$

where Δt is the time interval, $y_n = y(t_n)_{\,n=1,N}$, and $T = N\Delta t$. To find the variance associated with a given pair of harmonic predictors (C_k):

$$C_k = \frac{{A_k}^2 + {B_k}^2}{2}$$

C_k gives us the power values for the power spectrum. The power values for each spectrum were then normalized by dividing by the area comprised by the whole spectrum. For this to happen it first must be pointed out that by using this method, only half of the spectrum is retrieved as the second half is just a mirror image of the first half. Therefore, in order to be able to normalize each spectrum by dividing by the area of the whole spectrum, we must double the area of the first half of the spectrum. Since the focus of this study is on climate periodicities, each graph has an upper frequency limit of 0.04 year^{-1} or periodicity of 25 years.

In order to obtain significant peaks within the DFT power spectra, we must estimate an appropriate 95% confidence level. For this study the 95% confidence

aatsonis@uwm.edu

level was established by using 1000 Monte Carlo synthetic runs using fractional Brownian motions (fBms). It has been shown in the past (Koscielny-Bunde et al. 1998), and was verified here for all records, that temperature records do indeed have properties of fractional Brownian motions with an exponent (also referred to as the Hurst exponent) greater than 0.5. This is statistically desired because in this case surrogate data can be generated to assist in the statistical significance of the results. The Hurst Exponent can vary between 0.0 and 1.0. The range between 0.5 and 1.0 corresponds to persistence while the range between 0.0 and 0.5 corresponds to anti-persistence. First, in order to use fBms as surrogates, each temperature record must be examined to verify that it is indeed an fBm. To calculate the Hurst exponent (Feder 1988) of a time series:

$$y_n = y(t_n)_{n=1,N}$$

First, find the mean of the time series:

$$M = \frac{1}{N}\sum_{i=1}^{N} y_i$$

Then calculate the deviations from the mean:

$$\begin{aligned} x_1 &= y_1 - M \\ x_2 &= y_2 - M \\ &\cdots \\ x_n &= n - M \end{aligned}$$

Next, calculate the cumulative sums:

$$\begin{aligned} Z_1 &= x_1 \\ Z_2 &= x_1 + x_2 \\ &\cdots \\ Z_n &= \textstyle\sum_{i=1}^{n} x_i \end{aligned}$$

Compute the range:

$$R_n = \max[Z_n] - \min[Z_n]$$

Compute the standard deviation:

$$S_n = \sqrt{\frac{1}{n}\sum_{i=1}^{n}(y_i - M)^2}$$

The rescaling range $\frac{R_n}{S_n}$ can be used to estimate the Hurst exponent (H).

aatsonis@uwm.edu

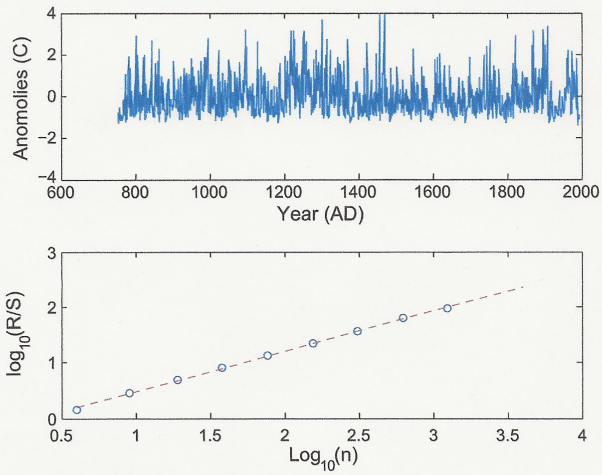

Fig. 1 Proxy record from Baffin Island, Canada (*top*) and its Hurst analysis (*bottom*). The results indicate that this record has properties of a fractional Brownian motion with an exponent of about 0.72

$$\frac{R_n}{S_n} = Cn^H$$

where C is a constant. From here:

$$\log\left(\frac{R_n}{S_n}\right) = \log(C) + H\log(n)$$

Then the slope of the linear regression line between $\log\left(\frac{R_n}{S_n}\right)$ $vs\log(n)$ gives the Hurst exponent H.

Figure 1 shows an example of the data used. It is from Baffin Island, Canada and it is a proxy sediment thickness record (top). The bottom graph shows the results of a Hurst analysis, which indicates that this record is indeed a fractional Brownian motion with an exponent of about 0.72 indicating persistence. We found that all the records used here are fBms with an exponent greater than 0.5. As was mentioned above, this result is consistent with earlier results base on temperature records (Koscielny-Bunde et al. 1998).

Figure 2 shows the statistical procedure used here to produce statistically significant periodicities in the data. First, the spectra of the proxy record were produced (blue line). Then we produced 1000 surrogate Brownian motion with

aatsonis@uwm.edu

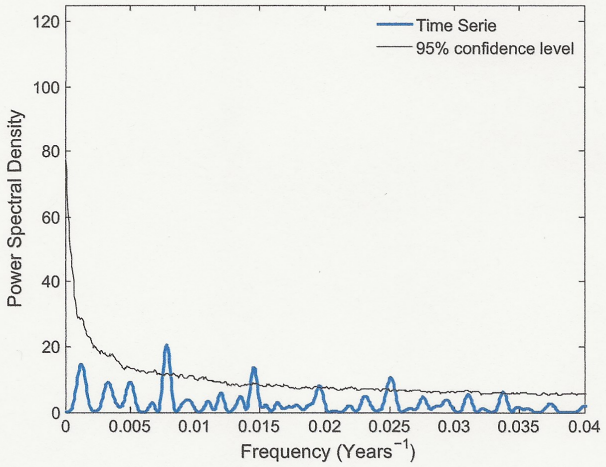

Fig. 2 Spectra of the proxy record in Fig. 2

the same exponent as the proxy data and calculated their spectra. Any peak in the original proxy data above the 95% percentile of these 1000 surrogates (black line) was then considered as a significant oscillation. In this case we have three significant oscillations at about frequencies 0.0075, 0.014, and 0.025 years^{-1} (or periodicities 130, 70, and 40 years). Figure 3 shows all the significant periodicities of all record but the last 5 (long interpolated records) and Fig. 4 shows all of the records (in red the last five very long records indicating astronomical Milankovitch forcing).

The important conclusion from this study is that there seems to exist two types of natural oscillations in the climate system. Those internal to the climate system ranging up to 1000 years and those of much longer period attributed to the Milankovitch cycles. There may still be oscillations in between but the data available here cannot resolve them. Yet the major conclusion is that long time-scale oscillations that cannot be attributed to human activity are present in proxy climate records.

This study is consistent with a much earlier study (Zhuang 1991), which used 13 different isotope records from the SPECMAP project http://gcmd.nasa.gov/records/GCMD_EARTH_LAND_NGDC_PALEOCL_SPECMAP.html (Fig. 5). The similarity between our results and those independent results is striking.

aatsonis@uwm.edu

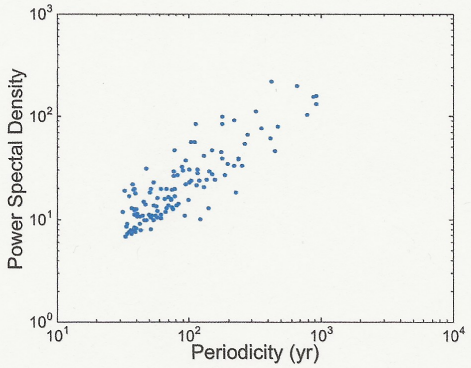

Fig. 3 Significant periodicities. All records but the last five

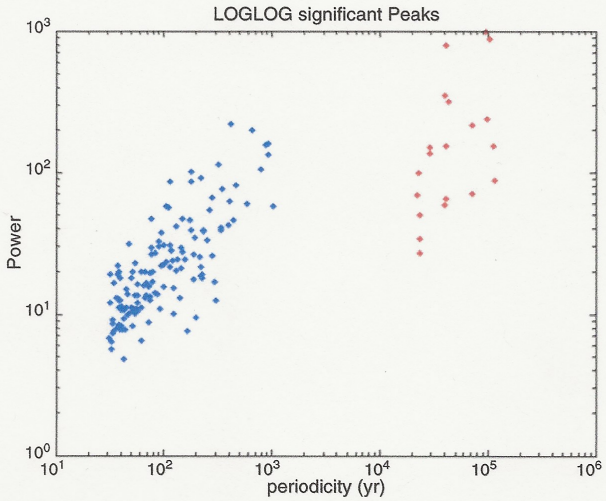

Fig. 4 Same as Fig. 3 but for all records

aatsonis@uwm.edu

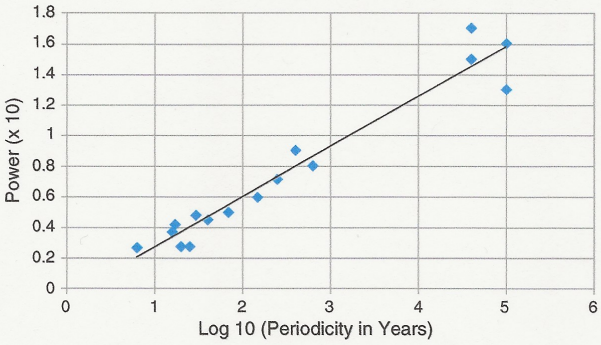

Fig. 5 Same as Fig. 4 but for an independent data set

References

Alley, R.B. 2004. *GISP2 ice core temperature and accumulation data. IGBP PAGES/World data center for paleoclimatology data contribution series #2004-013*. Boulder CO, USA: NOAA/NGDC Paleoclimatology Program.

Anchukaitis, K.J., R.D. D'Arrigo, L. Andreu-Hayles, D. Frank, A. Verstege, A. Curtis, B.M. Buckley, G.C. Jacoby, and E.R. Cook. 2013. Tree-ring-reconstructed summer temperatures from northwestern north america during the last nine centuries. *Journal of Climate* 26 (10): 3001–3012. doi:10.1175/JCLI-D-11-00139.1.

Auer, I., et al. 2007. HISTALP–historical instrumental climatological surface time series of the Greater Alpine Region. *International Journal of Climatology* 27: 17–46.

Bintanja, R., R.S.W. van de Wal, and J. Oerlemans. 2005. Modeled atmospheric temperatures and global sea levels over the past million years. *Nature* 437: 125–128. doi:10.1038/nature03975.

Biondi, F., et al. 2006. *East-central Idaho July Temperature Reconstruction. IGBP PAGES/World Data Center for Paleoclimatology Data Contribution Series # 2006-039*. Boulder CO, USA: NOAA/NCDC Paleoclimatology Program.

Büntgen, U., et al. 2013. Filling the Eastern European gap in millennium-long temperature reconstructions. *Proceedings of the National Academy of Sciences of the United States of America* 110 (5): 1773–1778. doi:10.1073/pnas.1211485110.

Climate Research Unit (CRU). 2012. *University of East Anglia (UK)*. Available at: http://www.metoffice.gov.uk/hadobs/crutem4/data/download.html

Czech Hydrometeorological Institute (CHMI). 2012. *143 06 Praha 4 Czech Republic*. Available at: http://zmeny-klima.ic.cz/klementinum-data/

Deutscher Wetterdienst (DWD). 2012. *Frankfurter Straße 135, 63067 Offenbach (Germany)*. Available at: www.dwd.de

Feder, J. 1988. *Fractals*. New York: Plenum Press.

Glaser, R., and D. Riemann. 2009. A thousand-year record of temperature variations for Germany and Central Europe based on documentary data. *Journal of Quaternary Science* 24: 437–449. ISSN 0267-8179. doi:10.1002/jqs.1302.

Grudd, H. 2008. Tornetrask tree-ring width and density AD 500-2004: a test of climatic sensitivity and a new 1500-year reconstruction of north Fennoscandian summers. *Climate Dynamics* 31: 843–857. doi:10.1007/s00382-007-0358-2.

aatsonis@uwm.edu

Gunnarson, B.E., H.W. Linderholm, and A. Moberg. 2011. Improving a tree-ring reconstruction from west-central Scandinavia: 900 years of warm-season temperatures. *Climate Dynamics* 36 (1–2): 97–108. doi:10.1007/s00382-010-0783-5.

Jouzel, J., et al. 2007. *EPICA Dome C Ice Core 800KYr Deuterium Data and Temperature Estimates. IGBP PAGES/World Data Center for Paleoclimatology Data Contribution Series # 2007-091*. Boulder CO, USA: NOAA/NCDC Paleoclimatology Program.

Kawamura, K., et al. 2007. *Dome Fuji Ice Core Preliminary Temperature Reconstruction, 0-340 kyr. IGBP PAGES/World Data Center for Paleoclimatology Data Contribution Series # 2007-074*. Boulder CO, USA: NOAA/NCDC Paleoclimatology Program.

Koscielny-Bunde, E., A. Bunde, S. Havlin, H.E. Roman, Y. Goldreich, and H.-J. Schellnhuber. 1998. Indication of a universal persistence law governing atmospheric variability. *Physical Review Letters* 31 (3): 729–732.

Loso, M.G. 2008. Summer temperatures during the Medieval Warm Period and Little Ice Age inferred from varved proglacial lake sediments in southern Alaska. *Journal of Paleolimnology* 41 (1): 117–128. doi:10.1007/s10933-008-9264-9.

Luckman, H., and R.J.S. Wilson. 2006. *Canadian Rockies Summer Temperature Reconstruction. IGBP PAGES/World Data Center for Paleoclimatology Data Contribution Series # 2006-011*. Boulder CO, USA: NOAA/NCDC Paleoclimatology Program.

Mangini, A., C. Spötl, and P. Verdes. 2005. Reconstruction of temperature in the Central Alps during the past 2000 yr from a d18O stalagmite record. *Earth and Planetary Science Letters* 235 (3–4): 741–751. doi:10.1016/j.epsl.2005.05.010.

Météo France. 2012. Available at: http://france.meteofrance.com

Moore, J.J., et al. 2003. *Baffin Island 1250 Year Summer Temperature Reconstruction, IGBP PAGES/World Data Center for Paleoclimatology Data Contribution Series # 2003-075*. Boulder CO, USA: NOAA/NGDC Paleoclimatology Program.

Petit, J.R., et al. 1999. Climate and Atmospheric History of the Past 420,000 years from the Vostok Ice Core, Antarctica. *Nature* 399: 429–436.

Schulz, M., and M. Mudelsee. 2002. REDFIT: estimating red-noise spectra directly from unevenly spaced paleoclimatic time series. *Computational Geosciences* 28: 421–426.

Shi, F., B. Yang, and L. Von Gunten. 2012. Preliminary multiproxy surface air temperature field reconstruction for China over the past millennium. *Science China Earth Sciences* 55 (12): 2058–2067. doi:10.1007/s11430-012-4374-7.

Sundqvist, H.S., K. Holmgren, J. Fohlmeister, Q. Zhang, M.M. Bar, C. Spitl, and H. Kirnich. 2013. Evidence of a large cooling between 1690 and 1740 AD in southern Africa. *Scientific Reports*. doi:10.1038/srep01767.

Tan, M., et al. 2003. *2650-Year Beijing Stalagmite Layer Thickness and Temperature Reconstruction, IGBP PAGES/World Data Center for Paleoclimatology Data Contribution Series # 2003-050*. Boulder CO, USA: NOAA/NGDC Paleoclimatology Program.

Trachsel, M., et al. 2012. Multi-archive summer temperature reconstruction for the European Alps, AD 1053–1996. *Quaternary Science Reviews* 46: 66–79. doi:10.1016/j.quascirev.2012.04.021.

Trachsel, M., M. Grosjean, D. Schnyder, C. Kamenik, and B. Rein. 2010. Scanning reflectance spectroscopy (380ñ730 nm): a novel method for quantitative high-resolution climate reconstructions from minerogenic lake sediments. *Journal of Paleolimnology* 44 (4): 979–994. doi:10.1007/s10933-010-9468-7.

Villalba, R., et al. 2006. *Southern Andes Temperature Reconstructions. IGBP PAGES/World Data Center for Paleoclimatology Data Contribution Series # 2006-024*. Boulder CO, USA: NOAA/NCDC Paleoclimatology Program.

Von Gunten, L., M. Grosjean, B. Rein, R. Urrutia, and P. Appleby. 2009. A quantitative high-resolution summer temperature reconstruction based on sedimentary pigments from Laguna Aculeo, central Chile, back to AD 850. *The Holocene* 19 (6): 873–881. doi:10.1177/0959683609336573.

Wilson, R., G. Wiles, R. DíArrigo, and C. Zweck. 2007. Cycles and shifts: 1,300 years of multi-decadal temperature variability in the Gulf of Alaska. *Climate Dynamics* 28: 425–440. doi:10.1007/s00382-006-0194-9.

aatsonis@uwm.edu

Yang, F., et al. 2013. Multi-proxy temperature reconstruction from the West Qinling Mountains, China, for the past 500 years. *PLoS One* 8 (2): e57638. doi:10.1371/journal.pone.0057638.
Zhuang, J. 1991. A study of the variability of the global climate system. Master of Science thesis, Department of Geosciences, University of Wisconsin-Milwaukee, USA.

aatsonis@uwm.edu